Intermittency in Nuclear Multifragmentation at Relativistic Energy

P. L. Jain, G. Singh, and M. S. El-Nagdy[a]

High Energy Experimental Laboratory, Department of Physics, State University of New York at Buffalo, Buffalo, New York 14260

(Received 22 August 1991)

The charge distribution of nuclear fragments for the nonfissile events of ^{238}U at 0.96A GeV in nuclear emulsion is fitted with a power law. The method of scaled factorial moments is used to study fluctuations in the nuclear fragmentations. An intermittent behavior is found in the data, but no clear evidence of critical phenomenon is observed in nuclear fragmentation.

PACS numbers: 25.75.+r, 24.60.Ky

The recent studies of intermittency [1] in particle and nuclear collisions have revealed a quite fruitful field of research, and in fact the study of fluctuations has led to interesting insights on physical phenomena. Moreover, the intermittency analysis in terms of scaled factorial moments in relation with percolation models has been shown to be relevant in the study of the nuclear multifragmentation process [2]. In nuclear collisions at lower bombarding energies ($< 1A$ GeV) particle production is strongly suppressed and nuclear breakup into fragments dominates. Fragment-size distributions exhibit similar features to those known in percolation models [3]. Thus heavy-ion collisions offer a unique opportunity to study new phases of nuclei. One phase is of a high-density high-temperature region around the quark-gluon plasma (hadron phase transition or a thermal transition at equilibrium). The other phase is the low-density moderate-temperature region near the liquid-gas phase transition, but not at equilibrium—a nonthermal process. One can study the transition by looking at the distribution in composition of the final products. Here we shall look at the nonthermal process.

In 1984, we did an analysis of nuclear interactions produced [4] in emulsion from ^{238}U projectile at 0.96A GeV, in which 51% of all the 894 interactions were due to fissionlike fragments with a cross section of $\sigma_F = 1755 \pm 82$ mb. Recently, considerable interest has centered around the idea of nuclear multifragmentation, so our interest in the present Letter is to analyze the remaining nonfissile events which broke up into multifragments. When a ^{238}U ion passes through the emulsion detector, the interactions in this medium were recorded up to ≈ 2.7 cm (corresponding to energy between 960 and 240), where various processes are competing which give rise to different charge spectra of the projectile fragments (PFs). The energy of the produced PFs is high enough to distinguish them easily from the target fragments [5]. In each event the charges of these projectile fragments were determined by a combination of different methods which included grain density, gap density, δ-ray counting, relative track widths, etc. [4]. For projectile fragments of heavy charges which stopped in the stack, we used relations between their thin down track length and the widths [6] which were developed from the data of standard stopping tracks by drawing the profile of their last (150–1000 μm) thin down track lengths with the help of a special Leitz "discussion tube" and comparing them with the profiles of unknown tracks of different charges. A heavy fragment here is defined as a cluster with charge greater than the α particle. While checking the charge conservation, the pions were eliminated from the angle given by the Fermi momentum [7] at each interaction point.

In Fig. 1(a) is shown the charge distribution of all the nonfissile fragments produced in 374 interactions from

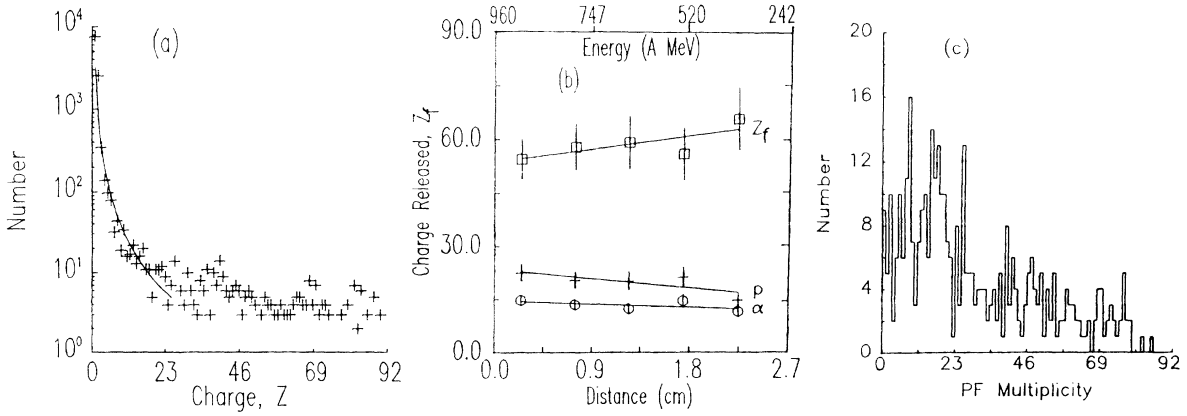

FIG. 1. (a) The charge distribution of all the fragments emerged in nonfissile events of ^{238}U in emulsion. For the solid curve, see text. (b) The charge released Z_f as a function of the energy. (c) The multiplicity distribution of the projectile fragments produced in nonfissile ^{238}U events.

$Z=1$ to 92. These estimates have an accuracy of ± 2 charge units. One of the remarkable features of the fragment charge distribution is the appearance of an inverse power law of the cluster size which fits to the fragment charge distribution and is shown in Fig. 1(a). The value of the exponent is -2.01 ± 0.09 up to $Z=25$. Power-law behaviors have also been seen in cluster-size distributions at the percolation threshold [8]. The energy dependences of the number of singly charged particles, mostly protons (N_p), of doubly charged helium nuclei (Z_α), and of the total charge released on heavy ($Z \geq 3$) fragments (Z_f) are shown in Fig. 1(b). It can be seen that Z_α is weakly dependent on energy as the energy varies from $960A$ to $240A$ MeV, and decreases linearly from $N_\alpha = 7.40 \pm 0.74$ to 5.78 ± 0.75 with $\langle N_\alpha \rangle = 6.70 \pm 0.35$. Similarly, N_p shows a linear decrease from 22.61 ± 2.25 to 14.85 ± 1.93 with an average $\langle N_p \rangle = 19.96 \pm 1.03$, which presumably represents mostly a decreasing degree of breakup. The average number of fragments with $Z \geq 3$ is 3.34 ± 0.17. The multiplicity distribution of all the charged fragments with $Z=1$ to 92 is shown in Fig. 1(c), and we find that for the PFs of multiplicity $27 \leq N_f \leq 80$ the average fragment multiplicity is $\langle N_f \rangle = 50.53 \pm 3.88$.

For intermittency to be present in the nuclear multifragmentation process, both scale invariance and random character of the scaling law are required. In multifragmentation, the charge distribution of the fragments [Fig. 1(a)] and the fragment multiplicity distribution [Fig. 1(c)] lead us to test the intermittency behavior in these two variables. For a physical system, the scaled factorial moment F_q of order q is calculated by [1]

$$\langle F_q \rangle = \frac{1}{\langle n_m \rangle^q} \left\langle \frac{1}{M} \sum_{m=1}^{M} n_m (n_m - 1) \cdots (n_m - q + 1) \right\rangle, \tag{1}$$

where

$$\langle n_m \rangle = \left\langle \frac{1}{M} \sum_{m=1}^{M} n_m \right\rangle$$

for events with mean fragment multiplicity $\langle n_m \rangle$ in the fragment charge interval Δs which is divided into M bins of size $\delta s = \Delta s / M$. The number of fragments in the mth bin ($m = 1, 2, \ldots, M$) is n_m. If self-similar fluctuations exist at all scales δs, the factorial moment of the order q is given by $\langle F_q \rangle = (\Delta s / \delta s)^{\alpha_q}$. The exponent α_q is the slope characterizing a linear rise of $\ln \langle F_q \rangle$ with $-\ln \delta s$ for all bins of δs. The exponent α_q increases with increasing order q of the moment; however, for a random uncorrelated particle production, $\langle F_q \rangle$ should be constant for all values of q. For nonflat fragments multiplicity distributions varying within a finite bin of width δs introduce an extra M-dependent correction factor R_q which is given by [9]

$$R_q = \frac{1}{M} \sum_{m=1}^{M} \frac{M^q \langle n_m \rangle^q}{\langle N_f \rangle^q}, \tag{2}$$

where

$$\langle n_m \rangle = \frac{1}{N_{\text{events}}} \sum_{i=1}^{N_{\text{event}}} n_{m,i}$$

and $\langle N_f \rangle$ is the average fragment multiplicity in the interval Δs. Thus, $\langle F_q \rangle / R_q = \langle F_q \rangle^{\text{corr}}$, which measures the properties of dynamical fluctuations. In doing so, one must be careful in selecting the smallest bin, which must not be smaller than the resolution of the detector as discussed in Ref. [10].

From Fig. 1(c), we selected a sample of 170 events with fragment multiplicity $0.29 < m < 0.87$ in the scaled units $m = N / N_{\max}$, where $N_{\max} = 92$ is the maximum possible number of fragments, and we applied the above technique. The distribution for $\langle F_q \rangle^{\text{corr}}$ is plotted as a function of $-\ln \delta s$ and this is exhibited in Fig. 2(a),

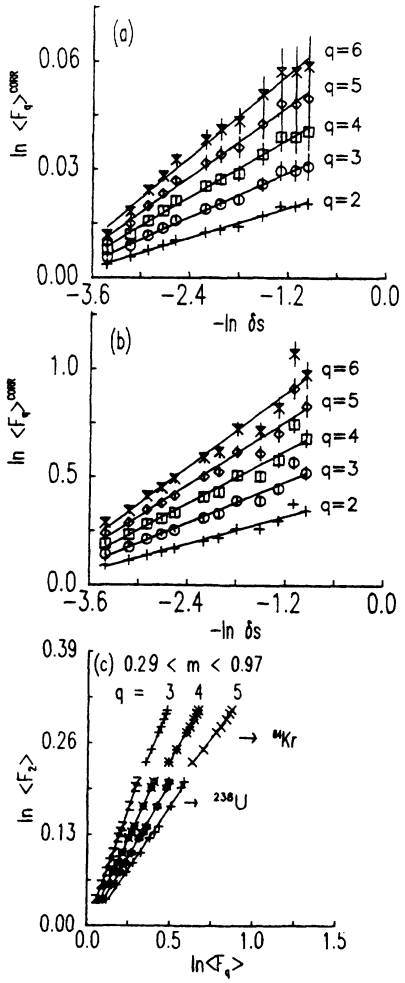

FIG. 2. (a) The variation of $\ln \langle F_q \rangle^{\text{corr}}$ as a function of $-\ln \delta s$ for the events with $0.29 < m < 0.87$. (b) The same plot as in (a), but for the events with $N_f \geq 3$ of charge $Z \geq 3$. (c) The variation of $\ln F_2$ as a function of $\ln F_q$ for ^{238}U ($q = 3$–6) and ^{84}Kr at $1.52A$ GeV ($q = 3$–5). The solid lines are the least-squares fits to the data points.

where the moments for the fragment multiplicity distribution continue to increase according to power law with decreasing bin width δs down to the experimental charge resolution. For the δs variable, the slopes α_q obtained from the least-squares fitting of the data points are $\alpha_2=0.0068\pm0.0002$, $\alpha_3=0.0102\pm0.0003$, $\alpha_4=0.0133\pm0.0004$, $\alpha_5=0.0163\pm0.0006$, $\alpha_6=0.0191\pm0.0006$, $\alpha_7=0.0216\pm0.0008$, and $\alpha_8=0.0239\pm0.0010$. They increase with the order q of the moments for all values of δs. We also selected 165 events with a large number of heavy fragments $N_f\geq3$ of charges $Z\geq3$ including protons and alpha particles. These are relatively soft collisions and the results for $\ln\langle F_q\rangle^{\rm corr}$ vs $-\ln\delta s$ are shown in Fig. 2(b). The slopes obtained from the least-squares fitting of the data points are $\alpha_2=0.1507\pm0.0055$, $\alpha_3=0.1573\pm0.0086$, $\alpha_4=0.2026\pm0.0117$, $\alpha_5=0.2448\pm0.0147$, $\alpha_6=0.2847\pm0.0176$, $\alpha_7=0.3156\pm0.0206$, and $\alpha_8=0.3524\pm0.0232$. The slopes in this case are much higher than in the previous case but in general they have the same characteristics as shown in Fig. 2(a). In both cases, the linear growth of the factorial moments clearly testifies to the presence of an intermittency pattern of the charge/mass distribution in the sample. The number of events in the present data is not large enough and does not allow us to do a more detailed study of the selection criteria for the critical events and especially those corresponding to narrow multiplicity bins of fragments. Recently, Ochs and Wosiek [11] have suggested that the moments of higher-order F_q are related to the second moments F_2 and they give important hints on the underlying dynamics. In Fig. 2(c), we have plotted $\ln F_2$ vs $\ln F_q$; the least-squares fits to the data points all meet approximately at one point giving the ratios $r_q=\ln F_q/\ln F_2=\alpha_q/\alpha_2$ as $r_3=1.6$, $r_4=2.3$, $r_5=3.1$, and $r_6=4.0$. These ratios of the slopes are weakly dependent on the reaction type and this can be seen when we plot the ratios r_q for the multifragmentation of ^{84}Kr at 1.52A GeV [12].

In Fig. 1(a), the observed multifragmentation process follows the power-law behavior near the critical point and such a nonthermal behavior has also been seen in the clustering-size distribution at the percolation threshold [8]. The power-law dependence may be considered as a necessary but not a sufficient proof for this transition. In order to check the presence of the critical phenomenon, we used a method which compares several quantities that behave in a qualitatively different way when a phase transition is present or not. These quantities are the conditional (second) moments which are enhanced in the multifragmentation region, provided that they are linked to a critical behavior. Second moments are given by [3] $M_2^j=\sum s^2 m^j(s)$, where $m^j(s)=0,1,2,\ldots,$ is the multiplicity of different fragments in the jth event. The sum runs over all fragments excluding the heaviest one produced in the event, and then it is normalized by $S_0=92$ (total charge of the breaking system) giving the normalized moment S_2^j. Campi [3] has investigated the conditional moments of the fragment-size distribution and shown that nuclei break up as a finite percolation network. In Fig. 3(a) is shown the relation between the normalized second moment $\langle\ln S_2\rangle$ and the multiplicity n, where n is the ratio of the number of charged fragments -1 (the maximum charged fragment, $Z_{\rm max}$) and the total charge $Z=92$. The third parameter is the fragment multiplicity which is divided into three groups, i.e., (a) soft, L_1 (3-27), (b) medium, L_2 (28-58), and (c) hard collisions, L_3 (59-92). The multiplicity cuts introduce restrictions on the available space in the figure. According to the percolation model [3] such a plot should give rise to two branches and both are observed in this figure. The maximum value of $\langle\ln S_2\rangle=6.0$ is at $n=0.29$. The broad maximum instead of a singularity is due to the finite size of the system. In Fig. 3(b) is plotted the charge of the largest fragment $\ln Z_{\rm max}$ vs the normalized second moment $\langle\ln S_2\rangle$ (excluding the largest charge) for L_1, L_2, and L_3 groups of particles. Once again, we observe two distinct branches. The highest multiplicity bin is only in the lower branch while the lowest multiplicity bin is in the upper branch and the events with high multiplicity are associated with low values of $Z_{\rm max}$. The fragments of the L_2 group contribute to both the branches. The events that fall in the critical region should then be created in a phase transition. Gross and co-workers [13] find the same curve in calculations based on a microscopic statistical model. In order to have a better insight into the shape of the fragment-size distribution, we examined the average behavior of relative variance $\langle\gamma_2\rangle$ as a func-

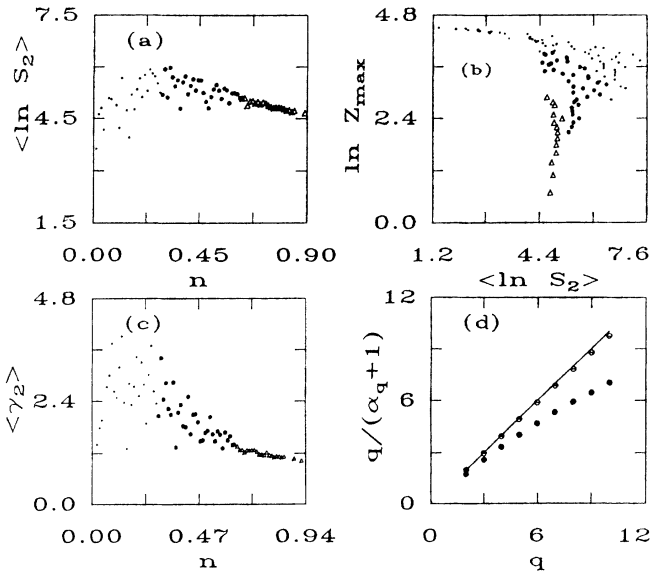

FIG. 3. (a) The plot of second moments $\langle\ln S_2\rangle$ vs n. (b) The variation of $\ln Z_{\rm max}$ as a function of $\langle\ln S_2\rangle$. (c) $\langle\gamma_2\rangle$ as a function of n for different multiplicity cuts. (d) The distribution of $q/(\alpha_q+1)$ as a function of q for the events of $0.29<m<0.87$ (open circles) and of events with $N_f\geq3$ of charge $Z\geq3$ (solid circles). The solid line corresponds to the condition $\alpha_q=0$ given in Eq. (3) (see text).

tion of the normalized multiplicity n, where $\langle\gamma_2\rangle = M_2 M_0 / M_1^2$, and this is shown in Fig. 3(c) with a maximum at $n \approx 0.22$. This distribution has proved to be a sensitive probe for a critical behavior where the projectile breaks up into two or three medium-sized fragments, thus giving the largest values of M_2. The fluctuations in the fragment-size distribution are largest near the critical point and the same is true in the finite system [14]. We also observed a linear and strong correlation when $\ln S_3$ is plotted against $\ln S_2$ (not shown here) giving the largest values in the critical region and this is also predicted by the percolation model [3]. From Figs. 3(a)–3(c) we conclude that there are strong similarities between the behavior of the data and the predictions of the finite-size percolation model when we study the correlations between $\ln Z_{\max}$, $\ln S_2$, $\langle\gamma_2\rangle$, and n.

The relationship between intermittency and statistical mechanics of disordered systems such as the spin-glass phase has lead Peschanski [15] to find the conditions for the nonthermal phase—as the new phase is not characterized by a thermodynamical behavior. It was further concluded [15] that these phase transitions involve the existence of a critical value q_c for the rank of the factorial intermittency moments $[\langle F_q\rangle^{\text{corr}}$ of Eq. (1)] for which one has

$$(\delta/\delta q)[q/(\alpha_q+1)]_{q=q_c}=0. \tag{3}$$

In Fig. 3(d) are plotted the slopes of factorial moments for the sample with $0.29 < m < 0.87$ and also with $N_f \geq 3$ of charge $Z \geq 3$. The solid line corresponds to $\alpha_q = 0$. Data points (open circles) for fragment multiplicity ($0.29 < m < 0.87$) are relatively close to the critical behavior satisfying the condition given by Eq. (3) while the data points (solid circles) for events with $N_f \geq 3$ of charge $Z \geq 3$ do not satisfy the condition (3) within the range of q values for which factorial moments and their slopes have been calculated [10].

We conclude that the fragment charge distribution of ^{238}U into a nonfissile multifragmentation process is fitted with a power law. Multifragmentation also gives evidence of an intermittency pattern of fluctuations and hence for self-similarity in the fragment-size distribution from a nuclear breakup process at $\approx 1A$ GeV. The experimental data and a percolation model of about the same dimension as shown in Figs. 3(a)–3(c) behave in a similar way and exhibit some evidence of a critical behavior. But, when the experimental data are compared with the predictions of Ref. [15] for an infinite system, the fluctuation patterns in the sample do not give any clear indication of a critical behavior.

We are thankful to the LBL technical staff for their help in the exposure of emulsion stacks. This work was supported by DOE under Grant No. DE-FG02-90ER40566.

[a]Permanent address: Department of Basic Science and Mathematics, Faculty of Petroleum, Suez Canal University, Suez, Egypt.

[1] A. Bialas and R. Peschanski, Nucl. Phys. **B273**, 703 (1986); **B308**, 857 (1988).

[2] M. Ploszajczak and A. Tucholski, Phys. Rev. Lett. **65**, 1539 (1990); P. Freier and J. Waddington, Phys. Rev. C **31**, 888 (1985).

[3] X. Campi, Phys. Lett. B **208**, 351 (1988); J. Phys. **19**, 917 (1986); B. Jacobsson *et al.*, Nucl. Phys. **A509**, 195 (1990).

[4] P. L. Jain, M. M. Aggarwal, M. S. El-Nagdy, and A. Z. M. Ismail, Phys. Rev. Lett. **52**, 1763 (1984).

[5] P. L. Jain, K. Sengupta, and G. Singh, Phys. Rev. C **44**, 844 (1991).

[6] P. L. Jain (unpublished).

[7] K. Sengupta, P. L. Jain, G. Singh, and S. N. Kim, Phys. Lett. B **236**, 219 (1989).

[8] D. Stauffer, Phys. Rep. **54**, 1 (1979).

[9] K. Fialkowski, B. Wosiek, and J. Wosiek, Acta Phys. Pol. B **20**, 639 (1989).

[10] P. L. Jain and G. Singh, Phys. Rev. C **44**, 854 (1991), and references therein.

[11] W. Ochs and J. Wosiek, Phys. Lett. B **214**, 617 (1988); Z. Phys. C **50**, 339 (1991).

[12] G. Singh, P. L. Jain, and M. S. El-Nagdy (to be published).

[13] Sa Ban-hao and D. H. E. Gross, Nucl. Phys. **A437**, 643 (1985); X. Z. Zhang and D. H. E. Gross, Nucl. Phys. **A461**, 641 (1987); **A461**, 668 (1987).

[14] H. E. Stanley, *Introduction to Phase Transition and Critical Phenomena* (Oxford Univ. Press, Oxford, 1987).

[15] R. Peschanski, Nucl. Phys. **B327**, 144 (1989).